HHS Public Access

Author manuscript

Behav Brain Res. Author manuscript; available in PMC 2018 March 30.

Published in final edited form as:

Behav Brain Res. 2017 March 30; 322(Pt B): 241–249. doi:10.1016/j.bbr.2016.06.054.

A novel mouse model of the aged brain: Over-expression of the L-type voltage-gated calcium channel $Ca_V1.3$

Jamie N. Krueger[a,d,*], **Shannon J. Moore**[a,*], **Rachel Parent**[a], **Brandon C. McKinney**[a,e], **Amy Lee**[c], and **Geoffrey G. Murphy**[a,b,‡]

[a]Molecular and Behavioral Neuroscience Institute, University of Michigan, Ann Arbor, MI 48109

[b]Department of Physiology, University of Michigan, Ann Arbor, MI 48109

[c]Molecular Physiology and Biophysics, University of Iowa, Iowa City, IA 52242

Abstract

The aged population is growing rapidly, which has sparked tremendous interest in elucidating mechanisms of aging in both the body and the brain. Animal models have become an indispensable tool in biomedical science, but because of the cost and extended timeframe associated with aging animals to appropriate time points, studies that rely on using aged animals are often not feasible. Somewhat surprisingly, there are relatively few animal models that have been specifically engineered to mimic physiological changes known to occur during “normal” aging. Developing transgenic animal models that faithfully mimic key aspects of aging would likely be of great utility in studying both age-related deficits in the absence of overt pathology as well as an adjunct for transgenic models of diseases where aging is a primary risk factor.

In particular, there are several alterations in the aged brain that are amenable to being modeled genetically. We have focused on one key aspect that has been repeatedly demonstrated in aged animals - an increase in the L-type voltage-gated calcium channel $Ca_V1.3$. Here we present a novel transgenic mouse line in which expression of $Ca_V1.3$ is increased by approximately 50% in the forebrain of young mice. These mice do not display any overt physical or non-cognitive deficits, exhibiting normal exploratory behavior, motor function, and affective-like responses, suggesting that these mice can be successfully deployed to assess the impact of an “aged brain” in a variety of conditions.

Keywords

aged brain; transgenic mice; L-type calcium channels; $Ca_V1.3$; neurobattery

[‡]Corresponding author: murphyg@umich.edu.
[d]Present address: Center for Neuroscience, University of California, Davis, Davis, CA 95618
[e]Present address: Department of Psychiatry and Translational Neuroscience Program, University of Pittsburgh, Pittsburgh, PA 15219
[*]Both authors contributed equally to this work

Introduction

As people age, they often experience declines in physical, physiological, and mental function which not only reduce the lifespan but also adversely impact the quality of life. The aged population is one of the fastest growing segments of society, which has been predicted to double in size by the year 2050, potentially representing over 20% of the total population in the United States [1]. As such, there has been increased interest in elucidating mechanisms that underlie age-related alterations so that potential therapeutic interventions can be identified and developed to ameliorate declining function.

Animal models have become an invaluable tool in biomedical science, and are used to study myriad aspects of biological mechanisms. Often, animal models are generated by introducing mutations into the genome to alter the function of target proteins or processes or to replicate mutations linked to specific human disease states. The “aged” phenotype, however, comprises a constellation of various changes throughout the body and brain that are complex and often interdependent, making it difficult to produce an accurate model. Thus, researchers interested in studying aging often have to literally “age” animals, simply waiting for them to reach a time point that is comparable to that of interest in humans. In the case of rodents, which are commonly used as animal models, this time point is generally 2–3 years, making this a very time-consuming and expensive experimental design.

One approach that has been taken in order to accelerate the time frame necessary for generating phenotypically aged mice is selective breeding. The senescence-accelerated-prone (SAMP) mouse lines were established by continuous interbreeding of littermates, which were selected on the basis of early senescence, shortened lifespan, and the development of age-associated pathologies, for many successive generations [2]. This process yielded a number of separate lines that each mimic specific characteristics of aged animals, including both physical deficits and cognitive deficits [3]. However, it is important to note that while these mice mimic some aspects of aging, it is difficult to determine whether the same mechanisms that underlie aging are contributing to the deficits observed in the SAMP mice. Thus, alterations in the expression, activity, and/or function of genes and proteins in the SAMP lines need to be validated by comparison to control mouse lines. While this represents a powerful unbiased method for identifying potential targets of interest, the selection of the “control” mouse line(s) introduces another significant caveat. Because the SAMP lines are a result of selective breeding, all mice in these lines are senescence-accelerated; therefore, there are no unaffected littermates to use as controls. Instead, control mice must be selected from other (genetically inbred) lines, each of which may have distinct mechanisms that contribute to an “aged” phenotype resulting in different catalogs of potential targets depending on the “control” chosen. A final crucial point is that each of the SAMP lines generally comprises multiple alterations that may contribute to the observed phenotypes. While this is similar to aging in which multiple factors likely interact to produce observed deficits, it confounds the understanding of the mechanism(s) responsible for specific age-related impairments. For example, the SAMP8 mouse line has garnered considerable interest because these mice exhibit cognitive deficits (particularly in learning and memory), which is a hallmark of aging in humans [4, 5]. However, these mice display both an increase in oxidative stress as well as an increase in amyloid beta [5],

making it is difficult to determine which mechanism is responsible for the deficits in learning and memory, and, moreover, to precisely elucidate the relative contribution of these processes to the cognitive decline that is observed in aged subjects.

In light of these limitations, our goal was to design a mouse model in which functional as well as mechanistic aspects of brain aging could be interrogated. There are many well-documented age-related changes that occur in the brain [6–8] and a number of these alterations could be modeled transgenically. We have chosen to focus our initial efforts on one key aspect of the aged brain: dysregulation of neuronal calcium (Ca^{2+}) homeostasis [9–11]. As a ubiquitous signaling molecule [12, 13], a crucial regulator of gene transcription [14, 15], and a critical modulator of both neuronal excitability [16] and plasticity [17], even small changes in Ca^{2+} homeostasis can significantly alter brain function. Several lines of evidence support the idea that Ca^{2+} homeostasis is dysregulated in the aged brain and that this contributes to age-related impairments in brain function (for example, the deficits in learning and memory that are often observed during aging), even in the absence of overt pathology. Calcium imaging experiments in the hippocampus showed that neurons from aged rats exhibited a significantly larger increase in intracellular Ca^{2+} concentration in response to depolarization than neurons from young rats [17]. This difference was only observed when the neurons fired action potentials, which suggested that the high voltage-activated class of voltage-gated calcium channels was involved [17]. Indeed, additional electrophysiological experiments demonstrated that the increase in whole-cell calcium currents was a result of an increase in the density of L-type voltage-gated calcium channels (L-VGCC) [18]. Further, the magnitude of the increase in calcium current and channel density was correlated with the degree of cognitive impairment in a hippocampus-dependent learning and memory task (the Morris water maze) [18]. Another line of evidence comes from electrophysiological recordings of the slow afterhyperpolarization (sAHP), a key determinant of neuronal excitability [19], which has been shown to require activation of L-VGCCs [20–23]. The sAHP in neurons from aged animals is significantly increased relative to that in young animals [24–27], consistent with the model of an increase in the number of available L-VGCCs that in turn activate more of the current underlying the sAHP. Interestingly, the magnitude of the sAHP recorded from hippocampal neurons has also been shown to be correlated with the degree of impairment in hippocampus-dependent learning and memory tasks (trace eyeblink conditioning and trace fear conditioning) – animals with a larger sAHP are impaired relative to those with a smaller sAHP [28, 29].

There are two primary L-VGCC pore forming subunits that are expressed in the mammalian brain: $Ca_V1.2$, which comprises ~80% of the total L-VGCC expression, and $Ca_V1.3$. While these subtypes have unique subcellular distributions [30], distinct electrophysiological properties [31], and have been implicated in different physiological roles [32], they cannot be differentiated by pharmacological agents. Thus, one approach that has been used to distinguish between the roles of these two L-VGCC subtypes is to generate transgenic mice lacking either $Ca_V1.2$ or $Ca_V1.3$. Previous work from our lab has suggested that the age-related increase in the sAHP is predominated by $Ca_V1.3$ because genetic deletion of $Ca_V1.3$ significantly reduces the magnitude of the sAHP [16, 33], whereas deletion of $Ca_V1.2$ does not appear to impact the sAHP [16]. Researchers have also used molecular and biochemical techniques to elucidate the contribution of the L-VGCC subtypes to the observed age-related

increase in calcium current and channel density. The majority of work, which has been performed in the hippocampus of rats, has revealed an increase in the amount of $Ca_V1.3$ mRNA [34, 35] and/or protein [36, 37], although recent evidence suggests that surface levels [38] and/or phosphorylation [38, 39] of $Ca_V1.2$ may be increased in some hippocampal subfields. However, single-cell analysis using reverse transcription polymerase chain reaction (RT-PCR) showed that the magnitude of the increase in $Ca_V1.3$ mRNA from individual hippocampal neurons correlated with the magnitude of the recorded calcium current [34], and additionally, the increase in $Ca_V1.3$ protein expression has been shown to be inversely correlated with the degree of impairment in the Morris water maze [37]. Further, aged mice, unlike aged rats, do not exhibit increased phosphorylation of $Ca_V1.2$ (at serine-1928), which can increase the calcium current mediated by this channel, nor do they exhibit changes in expression levels of $Ca_V1.2$ [27].

Taken together, the available evidence, especially in mice, strongly suggests that an increase in $Ca_V1.3$ is a primary contributor to the age-related dysregulation of neuronal calcium that underlies brain aging. In light of these observations, we have designed a novel line of transgenic mice that are engineered to over-express $Ca_V1.3$ in excitatory forebrain neurons, including the hippocampus and cortex. Here we describe the generation of these mice and their initial behavioral characterization, which demonstrates that they have no overt physical or non-cognitive deficits. Thus, we anticipate that these mice will be useful in studies investigating the putative role of $Ca_V1.3$ in “normal” brain aging as well as in studies aimed at determining the impact of age-related dysregulation of Ca^{2+} homeostasis on diseases in which age is a primary risk factor.

Materials and Methods

2.1 Transgene construction and generation of transgenic mice

The general cloning strategy is similar to that previously described [40, 41]. The original construct (sHA-$Ca_V1.3a$; a kind gift from I. Bezprozvanny, University of Texas Southwestern Medical Center, Dallas, TX) was provided in a pCDNA6/V5-hisB plasmid and contained the full length rat $Ca_V1.3$ cDNA that included a surface-expressed hemagglutinin (HA) epitope, which has previously been shown not to affect protein folding, trafficking to the cellular membrane, cell surface levels, or channel function [42, 43]. The pCDNA6/V5-hisB/sHA-$Ca_V1.3a$ plasmid was initially modified to replace the 5’ *NheI* site just adjacent to the ATG start codon with an *XmaI* site and a 3’ flanking *SacII* site was converted to an *FseI* site. These sites were used to excise the full length transgene, which was subsequently ligated into the multiple cloning site (MCS) of pNN265 that had been previously modified by the addition of a *XmaI* site 5’ adjacent to an existing *FseI* site. Thus, the resulting plasmid contained the full length $Ca_V1.3$HA transgene flanked by both a 5’ and a 3’ synthetic intron, which were included to help stabilize the mRNA and increase transgene expression during transcription [44]. In addition, the 3’ synthetic intron contained the a poly(A) signal from simian virus 40 necessary for mRNA translocation out of the nucleus. The $Ca_V1.3$ transgene and synthetic UTR sequences (a 7218bp fragment) were excised from the plasmid using two *NotI* sites that flanked the entire construct. This fragment was gel purified and subsequently cloned into a *NotI* site downstream of the full-

length (8.5kb) rat alpha Ca^{2+}/calmodulin-dependent protein kinase II (αCaMKII) promoter in vector pMM403 (both pNN265 and pMM403 were kindly provided by M. Mayford, The Scripps Research Institute, La Jolla, CA). We elected to use the αCaMKII promoter because it has been shown to effectively localize transgene expression to forebrain glutamatergic neurons [40, 41]. The resulting plasmid (pJNS01) containing the αCaMKII promoter, the 3' and 5' synthetic UTRs, and the $Ca_V1.3$HA sequence, was approximately 18 kb in size. Proper orientation of the transgene was confirmed by sequencing.

Approximately 50μg of pJNS01 was digested with *SfiI*, removing the pBS backbone fragment (3 kb) which originated from pMM403. The injection construct (15 kb), which included the αCaMKII promoter, synthetic UTRs, and $Ca_V1.3$HA cDNA (Figure 1A), was purified using the SNAP UV-Free Extraction Kit and sent to the University of Michigan Transgenic Core for pronuclear injection into fertilized C57BL/6 eggs that were then transferred into C57BL/6 pseudopregnant female mice.

2.2 Genotyping

Mice were genotyped for the presence of the $Ca_V1.3$HA transgene by polymerase chain reaction (PCR). After tail samples were digested overnight at 55°C in One-Step Tail Buffer (50mM KCl, 10mM Tris-HCl, 0.1% Triton X-100, 0.15mg/mL Proteinase K, pH 9.0), PCR was performed using GoTaq Green Master Mix (Promega, Madison, WI) with the following parameters: initial denaturation for 5:00 at 94°C, 30 cycles (0:30 at 94°C, 0:30 at 60°C, 1:00 at 72°C), and final elongation for 5:00 at 72°C. Primers for transgene were designed to span a ~350bp region in the synthetic 3' UTR (Figure 1A), which ensured that endogenous $Ca_V1.3$ DNA would not be detected. Primers for β-actin, spanning ~250bp, were also included as a control for the presence of DNA in the tail sample. Transgene primers were (CCACACCTCCCCCTGAACCTGAAACATAA) and (TGGAGGGTGTAATGAGTTCGGAGAC). Primers for β-actin were (CTCTCAGCTGTGGTGGTGAA) and (GCTCCCATTCATCAGTTCCATAGGT).

Mice that were genotyped as positive for the $Ca_V1.3$HA transgene are herein referred to as $Ca_V1.3$HA mice, and mice that were genotyped as negative for the $Ca_V1.3$HA transgene are referred to as wild-type (WT) mice. All mice were fed *ad libitum* and kept on a 14:10-hour light:dark schedule, with husbandry provided by the veterinarians and staff of the Unit for Laboratory Animal Medicine (ULAM) at the University of Michigan. Experimental procedures were approved by and performed in accordance with the University of Michigan Committee on Use and Care of Animals (UCUCA).

2.3 Western blot analysis

To detect the presence of the $Ca_V1.3$HA transgenic protein, Western blotting was performed on membrane fractions prepared from $Ca_V1.3$HA and WT littermate mice. After being deeply anesthetized using isoflurane (VetOne, Boise, ID), each mouse was decapitated and the brain was rapidly removed, bisected, and placed in a petri dish submerged in ice-cold phosphate-buffered saline (PBS; 20mM phosphate, 150mM NaCl, pH 7.4). The hippocampus, cortex, and cerebellum were isolated and placed in separate 1.5mL microcentrifuge tubes containing 500μL of ice-cold HEPES sucrose EDTA buffer (HSE;

10mM HEPES, 350mM Sucrose, 5mM ETDA) with a protease inhibitor (cOmplete; Roche Diagnostics, Indianapolis, IN). Samples were homogenized with a pestle and centrifuged at 6,000rpm at 4°C for 5 minutes. The resulting supernatant was then transferred to a 10.4mL ultracentrifuge tube containing HSE buffer, and centrifuged at 100,000 × *g* at 4°C for 1 hour. The supernatant was carefully removed, and the pellet was resuspended in 200μL HSE buffer with cOmplete protease inhibitor and 1% Triton X (Sigma-Aldrich, St. Louis, MO) to solubilize membranes proteins. Protein quantification was performed using the Bradford assay (Bio-Rad, Hercules, CA) with bovine serum albumin (BSA) as a standard. Samples were solubilized in Laemmli Buffer (Bio-Rad Hercules, CA), then boiled for five minutes at 95°C to denature the proteins. Proteins (20–30μg total protein loaded per lane) were separated on a 7.5% SDS-PAGE gel (Bio-Rad, Hercules, CA) run at 65V for 3 hours, and then transferred to a PVDF membrane overnight. To detect transgenic protein, the gel was first incubated overnight at 4°C with mouse anti-HA primary antibody (1:1000; Covance, Princeton, NJ), then washed 3 times for 10 minutes each in PBS with 0.1% Tween 20 (Sigma-Aldrich, St. Louis, MO), and finally incubated at room temperature for 1 hour with horseradish-peroxidase (HRP) conjugated goat anti-mouse secondary antibody (1:5000; Bio-Rad, Hercules, CA). Following additional washes (3 × 10 min in PBS with 0.1% Tween 20), immunoreactivity was visualized using Amersham Prime ECL (GE Healthcare, Waukesha, WI). To generate a loading control, the blot was then stripped and reprobed with mouse anti-transferrin primary antibody (1:500; Invitrogen, Carlsbad, CA) and HRP-conjugated goat anti-mouse secondary antibody (both using the same protocols as above). The blot was again visualized using Amersham Prime ECL.

To detect $Ca_V1.3$ protein (both endogenous and transgenic), Western blotting was performed on samples prepared from $Ca_V1.3$HA and WT littermate mice. After being deeply anesthetized using isoflurane, each mouse was decapitated, the brain was rapidly removed and then submerged in ice-cold artificial cerebrospinal fluid (aCSF, in mM: 120 NaCl, 3 KCl, 1.25 NaH_2PO_4, 25 $NaHCO_3$, 2.5 $CaCl_2$, 1 $MgSO_4$, 10 glucose, 0.4 ascorbic acid, pH 7.3). The forebrain was harvested, transferred to a Dounce tissue grinder containing 1mL ice-cold HSE buffer with cOmplete protease inhibitor, and homogenized. Homogenates were then centrifuged at 5,000rpm at 4°C for 5 minutes after which the supernatant was moved to a new tube and the pellet was discarded. Protein quantification was performed using the Bradford assay with BSA as a standard. Samples were solubilized in Laemmli Buffer and boiled for five minutes at 95°C to denature the proteins. Proteins (25μg of total protein loaded per lane) were separated on a 4–15% gradient SDS-PAGE gel (run at 65V for three hours) and then transferred to a PVDF membrane overnight. Before antibody incubation the membranes were cut at approximately 100kD; then, the section containing the larger proteins was incubated overnight at 4°C with rabbit anti-Cav1.3 primary antibody (1:3000; [45]), while the section containing the smaller proteins was incubated overnight at 4°C with rabbit anti-β-actin (1:2000; ThermoFisher Scientific, Wayne, MI), which served as a loading control. After primary antibody incubation, membranes were washed 3 times for 10 minutes each in PBS with 0.1% Tween 20, and then incubated at room temperature for 1 hour with HRP-conjugated goat anti-rabbit secondary antibody (1:5000; Milipore, Temecula, CA). Following additional washes (3 × 10 min in PBS with 0.1% Tween 20), immunoreactivity was visualized using Amersham Prime ECL (GE Healthcare, Waukesha, WI).

2.4 Neurobattery

At least one week before the start of behavioral characterization, mice were moved to a holding room near the behavior testing facilities so they could acclimate. The same cohort of mice, which consisted of $Ca_V1.3HA$ (n=13) and WT (n=18) littermates ranging in age from 3–5 months (average age: $Ca_V1.3HA$ = 3.5 ± 0.2mo, WT = 3.4 ± 0.1mo), was used for all of the behavioral testing. Experimenters were blind to the genotype of the mice during behavioral testing. All testing was performed at approximately the same time each day, during the animals' light cycle.

2.4.1 Open Field—The open field arena was a 71 × 71cm white acrylic box placed in a room lit by indirect white light. Mice were singly placed in the center of the box and allowed to explore for five minutes, during which time activity was recorded with LimeLight2 software (Actimetrics, Evanston, IL). The arena was thoroughly cleaned with 70% ethanol between each trial. For analysis, the arena was divided into an "edge" zone (a 10cm perimeter at the periphery of the arena, next to the wall) and a "center" zone, and distance traveled as well as time spent in each zone were computed by LimeLight2.

2.4.2 Light/Dark Box—The light/dark box was a 46 × 37cm rectangle made of acrylic placed in a room lit by indirect white light. The box was divided into two zones: a dark zone (approximately 1/3 of the total area), made of black acrylic with a black lid that remained closed, and a light zone (approximately 2/3 of the total area), which was made of white acrylic and was open at the top. A small opening in the center of the black acrylic wall separating the two zones allowed mice to cross from one zone into the other. Mice were singly placed in the center of the light zone and allowed to explore for five minutes, during which time activity was recorded with LimeLight2. The open field was thoroughly cleaned with 70% ethanol between trials for each animal. The percent time spent in each zone and the number of transitions (crossings) between the light and dark zones were analyzed using LimeLight2.

2.4.3 Rotarod—Mice were placed on a rotating rod that accelerated from 4 to 40 rpm over a five-minute time period (Stoelting, Chicago, IL) in groups of up to five (each cage of mice was run together, with 2–5 mice per cage), separated by dividers. Mice were given five trials over the course of one day, with approximately 1.5hr between each trial. Latency to fall was recorded by the experimenter, with a maximum of five minutes per trial.

2.5 Data Analysis

ImageJ (National Institutes of Health, Bethesda MD) was used to analyze pixel density of Western blot images. Data collected from behavioral experiments was analyzed with LimeLight2 software. StatView (SAS Institute Inc., Cary, NC) or GraphPad Prism 6 (GraphPad Software, Inc., La Jolla, CA) was used to calculate statistical significance (α =0.05) using Student's t-test, 2-factor ANOVA, or repeated measures ANOVA, as appropriate.

Results

An increase in expression of the L-VGCC, $Ca_V1.3$, has been repeatedly demonstrated in the brains of aged rodents [34–37] and is thought to represent a key aspect of the aged brain [9–11]. In order to determine the relative contribution of this alteration to age-related changes in brain function without the confounds of other pathologies associated with aging, we generated the $Ca_V1.3$HA transgenic mouse line to genetically mimic the age-related increase in $Ca_V1.3$. Here we describe the establishment and initial characterization of the $Ca_V1.3$HA transgenic mouse line, showing that there is an approximately 50% increase in $Ca_V1.3$ in forebrain regions and that these mice have normal baseline behavioral function. Thus these mice represent a useful genetic tool with which to investigate the mechanisms of brain function in a variety of physiological conditions and diseases that are impacted by aging.

3.1 Generation of injection construct and transgenic mouse lines

In order to generate transgenic mouse lines, we first synthesized an injection construct, which contained the HA-tagged $Ca_V1.3$ transgene flanked by synthetic 5’ and 3’UTR regions downstream of the αCaMKII promoter (Figure 1A). Importantly, the surface-expressed HA epitope (located on the extracellular side of domain II; Figure 1B) allows the transgenic protein ($Ca_V1.3$HA) to be distinguished from endogenous $Ca_V1.3$ protein and the positioning of the HA epitope in this region does not affect the cell surface levels or functional properties of the channel [42, 43]. The synthetic 5’ and 3’ UTRS were included because they have been shown to help stabilize mRNA and to increase transgene expression during transcription [44], and also to provide the poly-A sequence needed for mRNA translocation out of the nucleus. We chose to use the αCaMKII promoter for two main reasons: 1) the expression of αCaMKII (and therefore expression of the $Ca_V1.3$HA protein) peaks postnatally (around p7–p10) [46–48], which limits potential deleterious effects of transgenic protein expression during embryonic development ; and 2) the αCaMKII promoter has been shown to localize transgenic protein expression to excitatory forebrain neurons in transgenic animals [40, 48], which confines expression of $Ca_V1.3$HA protein to the population of neurons in which expression of $Ca_V1.3$ has been examined in aged rodents [34, 36, 37]. In addition, this minimizes the possibility that transgene expression in the cerebellum might interfere with normal motor function, which could confound behavioral tasks.

The linearized construct was sent to the University of Michigan Transgenic Core for pronuclear injection into fertilized eggs, which were then implanted into C57BL/6 pseudopregnant female mice. Out of 18 individual injection and implantation procedures, 6 pups (4 male, 2 female) that were genotyped as positive for the $Ca_V1.3$HA transgene ($Ca_V1.3$HA mice) were obtained. Each one of these $Ca_V1.3$HA mice (referred to as founders) was paired with a C57BL/6NTac mouse (Taconic Laboratories, Cambridge City, IN) of the opposite sex to establish individual mouse lines. The 2 female founders did not produce any viable progeny, but all 4 male founders produced pups that lived to be weaned. Of these, 3 of the 4 lines contained progeny that were genotyped as positive for the $Ca_V1.3$HA transgene. However, Western blot analysis detected $Ca_V1.3$HA transgenic protein expression in only 2 of these 3 lines (see below). Thus, this procedure has

established two viable transgenic mouse lines that express exogenous $Ca_V1.3$HA protein and therefore represent candidates for a mouse model of an aged brain (see Table 1).

3.2 Characterization of $Ca_V1.3$HA transgene expression

Our initial characterization efforts focused on $Ca_V1.3$HA mice from line 102. First, we determined the regional specificity of transgenic protein expression by Western blot analysis using an antibody against the HA epitope (anti-HA). To ensure that we were detecting $Ca_V1.3$HA transgenic protein that had been successfully folded, appropriately trafficked, and inserted into the plasma membrane, we prepared membrane fractions from cortex, hippocampus, and cerebellum of $Ca_V1.3$HA mice and their WT littermates. A band was detected at approximately 250kD (the same size as endogenous $Ca_V1.3$ protein) in both cortical and hippocampal, but not cerebellar, membrane fractions from $Ca_V1.3$HA but not WT mice (Figure 2A). This experiment demonstrates that transgenic protein expression is restricted to forebrain regions, due to the specificity of the αCaMKII promoter, and that the HA antibody specifically detects only transgenic, and not endogenous, protein.

While we predicted that transgene expression would result in an increase in total $Ca_V1.3$ protein, it is possible that endogenous $Ca_V1.3$ would be down-regulated in areas where the transgene was expressed, possibly as a result of a compensatory or homeostatic mechanism. Therefore, to measure total $Ca_V1.3$ protein levels, we performed Western blot analysis on whole brain samples (including cortex and hippocampus, but not cerebellum) using an antibody against $Ca_V1.3$ (anti-$Ca_V1.3$), which will identify both endogenous $Ca_V1.3$ and transgenic $Ca_V1.3$HA protein. A band was detected at approximately 250kD in both $Ca_V1.3$HA and WT mice, demonstrating the presence of $Ca_V1.3$ in both genotypes, but more protein was evident in the lane from $Ca_V1.3$HA mice (Figure $2B_1$). This strongly suggests that expression of the $Ca_V1.3$HA transgene did not cause down-regulation of endogenous $Ca_V1.3$ protein and instead resulted in an increase in total $Ca_V1.3$ protein.

Finally, to quantify the increase in $Ca_V1.3$ expression in transgenic mice, Western blots were performed on whole-brain samples (including cortex and hippocampus, but not cerebellum) from five $Ca_V1.3$HA mice and five WT littermates. Blots were probed with anti-$Ca_V1.3$ (which will detect both transgenic protein and endogenous protein) and with anti-β-actin (to serve as a loading control). The resulting blot was subjected to densitometric analysis using ImageJ software whereby the pixel density of each protein band ($Ca_V1.3$ and β-actin) was measured. Then the ratio of the $Ca_V1.3$ band to the β-actin band ($Ca_V1.3$: β-actin) was normalized to the average $Ca_V1.3$: β-actin ratio for all the WT samples. This analysis revealed that there was a significant increase in $Ca_V1.3$ protein expression in $Ca_V1.3$HA mice, relative to their WT littermates, of approximately 50% ($p < 0.05$, Student's t-test; Figure $2B_2$).

3.3 Initial behavioral characterization of the $Ca_V1.3$HA transgenic mouse line

In addition to the Western blot analysis described above, a separate cohort containing $Ca_V1.3$HA (n=13) and WT (n=18) littermate mice was characterized in a series of standard neurobattery tests to determine whether $Ca_V1.3$ transgene expression resulted in any overt alterations in exploration, locomotion, anxiety-like behavior, or motor learning.

3.3.1 Open Field—The open field test was performed to assess overall exploratory and anxiety-like behavior. Mice were individually placed in the open field for a five-minute trial, during which they were allowed to freely explore the arena while being recorded with LimeLight2 tracking software. Subsequent analysis revealed no difference between groups in the total distance traveled (Figure $3A_1$), suggesting that expression of the $Ca_V1.3$ transgene did not affect exploratory behavior and that $Ca_V1.3HA$ mice are neither hyper- nor hypo-mobile. Further, dividing the arena into an "edge" zone (by the arena wall) and "center" zone showed that although both $Ca_V1.3HA$ and WT mice spent significantly more time in the "edge" zone (which is typical behavior for mice, who generally avoid open spaces), there was no difference between genotypes in the amount of time spent in either zone (Figure $3A_2$), suggesting $Ca_V1.3HA$ mice do not exhibit altered anxiety-like behavior.

3.3.2 Light/Dark Box—While both exploratory and anxiety-like behavior can be assayed in the open field test, the light/dark box is generally considered a more sensitive measure of anxiety. Therefore, the $Ca_V1.3HA$ and WT mice were also assessed in the light/dark box, where each mouse received a five-minute trial during which they were allowed to freely explore the arena while being recorded with LimeLight2 tracking software. Similar to the results from open field, although both $Ca_V1.3HA$ and WT mice spent significantly more time on the dark side compared to the light side of the box (which is also typical behavior for mice, who generally avoid brightly lit spaces), there was no difference between genotypes in the amount of time spent in either the light or dark areas (Figure $3B_1$) or in the number of crossings between the light and dark sides (Figure $3B_2$). These data provide further strong evidence that $Ca_V1.3HA$ mice, like WT mice, prefer closed, dark spaces but are willing to explore other areas to a similar extent as their WT counterparts, and thus do not exhibit over- or under-exaggerated anxiety-like behavior.

3.3.3 Rotarod—The accelerating rotarod was used to assess both gross locomotor function as well as motor learning. $Ca_V1.3HA$ and WT cagemates were placed on a slowly (4rpm) rotating rod, separated by dividers. Over a 5-minute (300s) period, the rotation speed accelerated from 4 to 40rpm, and the latency to fall off the rod was recorded. Mice were given 5 trials in 1 day, with an inter-trial interval of approximately 1.5 hours. Performance (latency to fall) on the first trial was not different between genotypes, indicating that $Ca_V1.3HA$ mice have normal gross locomotor function (Figure 3C). Additionally, over the course of training, both $Ca_V1.3HA$ and WT mice exhibited a significant increase in latency to fall, but their performance was not different from each other, which demonstrates that mice in both groups display normal motor learning. These results are consistent with our Western blot analysis showing that expression of the transgenic protein was restricted to the forebrain by the αCamKII promoter as the cerebellum is critically involved in both locomotor performance and motor learning. Finally, because body weight can affect motor performance and differences may occlude the observation of a behavioral phenotype, a subset of mice used in neurobattery experiments were weighed after completion of the rotarod task (Figure 3D). There was no significant difference in weight between the $Ca_V1.3HA$ and WT mice, further suggesting that expression of the $Ca_V1.3$ transgene does not result in any gross physical defects or deficits in motor function.

Discussion

The transgenic model of an aged brain presented here has several distinct advantages over obtaining aged mice from suppliers or aging mice in-house. Perhaps the most practical concerns are cost and time. Buying aged mice from suppliers is often prohibitively expensive, and while aged mice can be obtained from some institutions at little to no cost (e.g. National Institute on Aging), there are restrictions on the number of mice available to investigators. Further, only wild-type mice are available, so it is not possible to use these resources to examine aged mice that have been genetically modified or treated with pharmacological agents. Instead, researchers must bred their own mice, or at least obtain transgenic or treated mice at substantially younger ages, and then age them in their own facilities, which requires paying per diem costs for mouse housing and husbandry (typically $0.70 – $1.00 a day per cage) that can exceed $500 for a single cage of 24-month old mice. This cost is compounded by the fact that not all mice will survive to the 24-month mark, thus requiring an additional allocation of mice (often 50% or more of the total number needed for the experiment) simply to account for mouse mortality. Considering that each experiment therefore requires 5–10 cages of mice per condition, the total cost for one experiment can easily exceed several thousand dollars. Additionally, breeding mice to be used for studies that involve aging, by definition, takes many months or years so it can be difficult and time-consuming to test different experimental manipulations. Therefore, using a transgenic model of an aged brain means that mice can be used at much younger ages, saving time and money, as well as allowing a greater extent of freedom in investigating multiple experimental manipulations.

Of course, “aging” is a complicated and multifaceted process, comprising myriad changes in the body and the brain. Because studying only one aspect of aging in isolation does not reproduce the entire aging milieu, it may be argued that this approach will yield limited insight into the function of the aged brain. However, precisely because “aging” encompasses a large number of variables, even with well-controlled experiments that focus on individual aspects, it is difficult to enumerate the relative contribution of distinct mechanisms to age-related alterations and to elucidate potential therapeutic targets that may ameliorate declines in function. For example, there is substantial interest in identifying mechanisms that contribute to age-related cognitive decline – especially impairments in learning and memory – which has been repeatedly demonstrated in humans, non-human primates, and rodents [4, 49]. In elderly human subjects, cognitive capacity can be determined using a wide variety of assessment tools [50], but most utilize verbal assessment (e.g. mini mental state exam). In contrast, almost all of the behavioral tasks that have been developed to study cognition in animal models like mice require some form of motor output (or suppression of motor output). Although we and others typically go to great lengths to control for deficits in motor ability and/or alterations in emotional reactivity, it is difficult if not impossible to completely remove the inherent confounds of using aged animals on the interpretation of cognitive performance. Therefore, the lack of any phenotypic deficits in the neurobattery of the $Ca_V1.3$HA mice compared to their WT littermates represents an important advantage of this model in that future studies utilizing these mice will not be confounded by other age-related

changes that may confuse or obscure the interpretation of experimental results in the context of cognitive function.

One of the biggest advantages of the $Ca_V1.3$HA transgenic mouse line is that it can be combined with other mouse models that emulate distinct aspects of normal aging or pathology to investigate the impact of an aged brain in a variety of conditions. For example, advancing age is the leading risk factor for many neurodegenerative disorders, including Alzheimer's disease (AD), Parkinson's disease (PD), and Huntington's disease (HD) [51–53]. However, because of the time and cost of aging animals to time points that would be comparable to the average age of disease onset in humans (e.g. approximately 2 years or more in rodents), many studies utilize genetic models of disease that are designed to be aggressive and manifest at relatively young ages (e.g. 2–6 months in rodents), which then lack important aspects of the aged phenotype that may fundamentally contribute to the disease in humans. While this approach has provided important information about some of the mechanisms involved, it remains likely that the brain environment (i.e. a "young brain" versus an "aged brain") substantially impacts the initiation, progression, and cognitive outcomes associated with these diseases. Thus, using the $Ca_V1.3$HA mouse line as a background on which to investigate the cellular and molecular mechanisms will likely provide a more representative and comprehensive understanding of these diseases. In addition, transgenic mouse models that mimic different age-related insults, such as an increase in reactive oxygen species (ROS) [54–56], changes in vascular function [57–60], or disrupted cholinergic signaling [61–64], could be crossed with $Ca_V1.3$HA mice to investigate the impact of interactions between different age-related alterations on cognitive outcomes. Taken together, the $Ca_V1.3$HA transgenic mouse line represents a significant step forward in the development of methodologies that will allow consideration of crucial aspects of the aged brain on both "normal" aging and in pathological conditions, improving our understanding of these processes and elucidating potential therapeutic interventions to ameliorate age-related cognitive decline.

Conclusions

We have successfully generated a novel transgenic mouse line in which expression of the L-VGCC subtype $Ca_V1.3$ is increased by approximately 50% in forebrain tissue, which mimics a key aspect of the aged brain. Notably, the transgenic $Ca_V1.3$ protein includes a surface-expressed HA epitope, which allows endogenous $Ca_V1.3$ to be distinguished from transgenic $Ca_V1.3$ protein. Importantly, mice positive for the transgene ($Ca_V1.3$HA mice) exhibit no gross exploratory, locomotor, or non-cognitive deficits compared to their WT littermates, suggesting that their performance in behavioral tasks can be successfully assessed without being impacted by other age-related pathologies. Thus, $Ca_V1.3$HA mice represent a promising model that will facilitate studies in which age is an important factor without the time, expense, and additional confounds associated with directly aging animals. We anticipate that the use of $Ca_V1.3$HA mice in future studies, either independently or in concert with other transgenic mouse models, will provide new insights into the mechanisms underlying the disruption of cognitive function that occurs with "normal" aging or in combination with other age-related diseases.

Acknowledgments

The authors wish to thank Dr. Mark Mayford and Dr. Ilya Bezprozvanny for their generous gifts of plasmids. This work was funded by NIH (to GGM: R01AG052934 and R01AG028488; to AL: NS084190, DC009433) and the University of Michigan Endowment for Basic Science.

References

1. Cesari, MJ. The demographic transition of the United States. Hauppauge, N.Y.: Nova Science Publishers; 2011.
2. Hosokawa M, Abe T, Higuchi K, Shimakawa K, Omori Y, Matsushita T, et al. Management and design of the maintenance of SAM mouse strains: an animal model for accelerated senescence and age-associated disorders. Exp Gerontol. 1997; 32:111–116. [PubMed: 9088908]
3. Takeda T. Senescence-accelerated mouse (SAM): a biogerontological resource in aging research. Neurobiol Aging. 1999; 20:105–110. [PubMed: 10537019]
4. Barnes CA. Aging and the physiology of spatial memory. Neurobiol Aging. 1988; 9:563–568. [PubMed: 3062467]
5. Butterfield DA, Poon HF. The senescence-accelerated prone mouse (SAMP8): a model of age-related cognitive decline with relevance to alterations of the gene expression and protein abnormalities in Alzheimer's disease. Exp Gerontol. 2005; 40:774–783. [PubMed: 16026957]
6. Blalock EM, Chen KC, Sharrow K, Herman JP, Porter NM, Foster TC, et al. Gene microarrays in hippocampal aging: statistical profiling identifies novel processes correlated with cognitive impairment. J Neurosci. 2003; 23:3807–3819. [PubMed: 12736351]
7. Kadish I, Thibault O, Blalock EM, Chen KC, Gant JC, Porter NM, et al. Hippocampal and cognitive aging across the lifespan: a bioenergetic shift precedes and increased cholesterol trafficking parallels memory impairment. J Neurosci. 2009; 29:1805–1816. [PubMed: 19211887]
8. Rowe WB, Blalock EM, Chen KC, Kadish I, Wang D, Barrett JE, et al. Hippocampal expression analyses reveal selective association of immediate-early, neuroenergetic, and myelinogenic pathways with cognitive impairment in aged rats. J Neurosci. 2007; 27:3098–3110. [PubMed: 17376971]
9. Foster TC, Kumar A. Calcium dysregulation in the aging brain. Neuroscientist. 2002; 8:297–301. [PubMed: 12194497]
10. Khachaturian, ZS. Toward theories of brain aging. In: Kay, DWK., Burrows, GD., editors. Handbook of studies on psychiatry and old age. Amsterdam: Elsevier; 1984. p. 7-30.
11. Khachaturian, ZS., Cotman, CW., Pettegrew, JW. Calcium, membranes, aging, and Alzheimer's disease. New York, N.Y.: New York Academy of Sciences; 1989. John Douglas French Foundation for Alzheimer's Disease., Pharmaceutical Manufacturers Association., National Institute on Aging.
12. Clapham DE. Calcium signaling. Cell. 2007; 131:1047–1058. [PubMed: 18083096]
13. Simms BA, Zamponi GW. Neuronal voltage-gated calcium channels: structure, function, and dysfunction. Neuron. 2014; 82:24–45. [PubMed: 24698266]
14. Barbado M, Fablet K, Ronjat M, De Waard M. Gene regulation by voltage-dependent calcium channels. Biochim Biophys Acta. 2009; 1793:1096–1104. [PubMed: 19250948]
15. Alonso MT, Garcia-Sancho J. Nuclear Ca(2+) signalling. Cell Calcium. 2011; 49:280–289. [PubMed: 21146212]
16. Gamelli AE. Deletion of the L-type calcium channel $Ca_V1.3$ but not $Ca_V1.2$ results in a diminished sAHP in mouse CA1 pyramidal neurons. Hippocampus. 2011; 21:133–141. [PubMed: 20014384]
17. Thibault O, Hadley R, Landfield PW. Elevated postsynaptic $[Ca^{2+}]_i$ and L-type calcium channel activity in aged hippocampal neurons: relationship to impaired synaptic plasticity. J Neurosci. 2001; 21:9744–9756. [PubMed: 11739583]
18. Thibault O, Landfield PW. Increase in single L-type calcium channels in hippocampal neurons during aging. Science. 1996; 272:1017–1020. [PubMed: 8638124]
19. Madison DV, Nicoll RA. Control of the repetitive discharge of rat CA 1 pyramidal neurones in vitro. J Physiol. 1984; 354:319–331. [PubMed: 6434729]

20. Bowden SE, Fletcher S, Loane DJ, Marrion NV. Somatic colocalization of rat SK1 and D class (CaV1.2) L-type calcium channels in rat CA1 hippocampal pyramidal neurons. J Neurosci. 2001; 21:RC175. [PubMed: 11588205]
21. Lima PA, Marrion NV. Mechanisms underlying activation of the slow AHP in rat hippocampal neurons. Brain Res. 2007; 1150:74–82. [PubMed: 17395164]
22. Marrion NV, Tavalin SJ. Selective activation of Ca^{2+}-activated K^+ channels by co-localized Ca^{2+} channels in hippocampal neurons. Nature. 1998; 395:900–905. [PubMed: 9804423]
23. Goldberg JA, Wilson CJ. Control of spontaneous firing patterns by the selective coupling of calcium currents to calcium-activated potassium currents in striatal cholinergic interneurons. J Neurosci. 2005; 25:10230–10238. [PubMed: 16267230]
24. Moyer JR Jr, Thompson LT, Black JP, Disterhoft JF. Nimodipine increases excitability of rabbit CA1 pyramidal neurons in an age- and concentration-dependent manner. J Neurophysiol. 1992; 68:2100–2109. [PubMed: 1491260]
25. Landfield PW, Pitler TA. Prolonged Ca^{2+}-dependent afterhyperpolarizations in hippocampal neurons of aged rats. Science. 1984; 226:1089–1092. [PubMed: 6494926]
26. Power JM, Wu WW, Sametsky E, Oh MM, Disterhoft JF. Age-related enhancement of the slow outward calcium-activated potassium current in hippocampal CA1 pyramidal neurons in vitro. J Neurosci. 2002; 22:7234–7243. [PubMed: 12177218]
27. Murphy GG, Shah V, Hell JW, Silva AJ. Investigation of age-related cognitive decline using mice as a model system: neurophysiological correlates. Am J Geriatr Psychiatry. 2006; 14:1012–1021. [PubMed: 17138808]
28. Moyer JR Jr, Power JM, Thompson LT, Disterhoft JF. Increased excitability of aged rabbit CA1 neurons after trace eyeblink conditioning. J Neurosci. 2000; 20:5476–5482. [PubMed: 10884331]
29. Kaczorowski CC, Disterhoft JF. Memory deficits are associated with impaired ability to modulate neuronal excitability in middle-aged mice. Learn Mem. 2009; 16:362–366. [PubMed: 19470651]
30. Hell JW, Westenbroek RE, Warner C, Ahlijanian MK, Prystay W, Gilbert MM, et al. Identification and differential subcellular localization of the neuronal class C and class D L-type calcium channel alpha 1 subunits. J Cell Biol. 1993; 123:949–962. [PubMed: 8227151]
31. Xu W, Lipscombe D. Neuronal Ca(V)1.3alpha(1) L-type channels activate at relatively hyperpolarized membrane potentials and are incompletely inhibited by dihydropyridines. J Neurosci. 2001; 21:5944–5951. [PubMed: 11487617]
32. Zamponi GW, Striessnig J, Koschak A, Dolphin AC. The Physiology, Pathology, and Pharmacology of Voltage-Gated Calcium Channels and Their Future Therapeutic Potential. Pharmacol Rev. 2015; 67:821–870. [PubMed: 26362469]
33. McKinney BC, Sze W, Lee B, Murphy GG. Impaired long-term potentiation and enhanced neuronal excitability in the amygdala of CaV1.3 knockout mice. Neurobiol Learn Mem. 2009; 92:519–528. [PubMed: 19595780]
34. Chen KC, Blalock EM, Thibault O, Kaminker P, Landfield PW. Expression of α_{1D} subunit mRNA is correlated with L-type Ca^{2+} channel activity in single neurons of hippocampal "zipper" slices. Proc Natl Acad Sci U S A. 2000; 97:4357–4362. [PubMed: 10759553]
35. Herman JP, Chen KC, Booze R, Landfield PW. Up-regulation of α_{1D} Ca^{2+} channel subunit mRNA expression in the hippocampus of aged F344 rats. Neurobiol Aging. 1998; 19:581–587. [PubMed: 10192218]
36. Veng LM, Browning MD. Regionally selective alterations in expression of the α_{1D} subunit ($Ca_V1.3$) of L-type calcium channels in the hippocampus of aged rats. Brain Res Mol Brain Res. 2002; 107:120–127. [PubMed: 12425941]
37. Veng LM, Mesches MH, Browning MD. Age-related working memory impairment is correlated with increases in the L-type calcium channel protein α_{1D} ($Ca_V1.3$) in area CA1 of the hippocampus and both are ameliorated by chronic nimodipine treatment. Brain Res Mol Brain Res. 2003; 110:193–202. [PubMed: 12591156]
38. Nunez-Santana FL, Oh MM, Antion MD, Lee A, Hell JW, Disterhoft JF. Surface L-type Ca^{2+} channel expression levels are increased in aged hippocampus. Aging Cell. 2014; 13:111–120. [PubMed: 24033980]

39. Davare MA, Hell JW. Increased phosphorylation of the neuronal L-type Ca^{2+} channel $Ca_V1.2$ during aging. Proc Natl Acad Sci U S A. 2003; 100:16018–16023. [PubMed: 14665691]
40. Mayford M, Bach ME, Huang YY, Wang L, Hawkins RD, Kandel ER. Control of memory formation through regulated expression of a CaMKII transgene. Science. 1996; 274:1678–1683. [PubMed: 8939850]
41. Kushner SA, Elgersma Y, Murphy GG, Jaarsma D, van Woerden GM, Hojjati MR, et al. Modulation of presynaptic plasticity and learning by the H-ras/extracellular signal-regulated kinase/synapsin I signaling pathway. J Neurosci. 2005; 25:9721–9734. [PubMed: 16237176]
42. Zhang H. $Ca_V1.2$ and $Ca_V1.3$ neuronal L-type calcium channels: differential targeting and signaling to pCREB. The European journal of neuroscience. 2006; 23:2297–2310. [PubMed: 16706838]
43. Altier C, Dubel SJ, Barrere C, Jarvis SE, Stotz SC, Spaetgens RL, et al. Trafficking of L-type calcium channels mediated by the postsynaptic scaffolding protein AKAP79. J Biol Chem. 2002; 277:33598–33603. [PubMed: 12114507]
44. Callis J. Introns increase gene expression in cultured maize cells. Genes & development. 1987; 1:1183–1200. [PubMed: 2828168]
45. Gregory FD, Bryan KE, Pangrsic T, Calin-Jageman IE, Moser T, Lee A. Harmonin inhibits presynaptic Cav1.3 Ca(2)(+) channels in mouse inner hair cells. Nat Neurosci. 2011; 14:1109–1111. [PubMed: 21822269]
46. Burgin KE, Waxham MN, Rickling S, Westgate SA, Mobley WC, Kelly PT. In situ hybridization histochemistry of Ca2+/calmodulin-dependent protein kinase in developing rat brain. J Neurosci. 1990; 10:1788–1798. [PubMed: 2162385]
47. Liu W, Chang L, Song Y, Gao X, Ling W, Lu T, et al. Immunolocalization of CaMKII and NR2B in hippocampal subregions of rat during postnatal development. Acta Histochem. 2013; 115:264–272. [PubMed: 22906554]
48. Hanson PI, Schulman H. Neuronal Ca2+/calmodulin-dependent protein kinases. Annu Rev Biochem. 1992; 61:559–601. [PubMed: 1323238]
49. Cognitive Aging: Progress in Understanding and Opportunities for Action. Washington D.C.: 2015.
50. Woodford HJ, George J. Cognitive assessment in the elderly: a review of clinical methods. QJM. 2007; 100:469–484. [PubMed: 17566006]
51. Bishop NA, Lu T, Yankner BA. Neural mechanisms of ageing and cognitive decline. Nature. 2010; 464:529–535. [PubMed: 20336135]
52. Douglas PM, Dillin A. Protein homeostasis and aging in neurodegeneration. J Cell Biol. 2010; 190:719–729. [PubMed: 20819932]
53. Reeve A, Simcox E, Turnbull D. Ageing and Parkinson's disease: why is advancing age the biggest risk factor? Ageing Res Rev. 2014; 14:19–30. [PubMed: 24503004]
54. Massaad CA, Klann E. Reactive oxygen species in the regulation of synaptic plasticity and memory. Antioxid Redox Signal. 2011; 14:2013–2054. [PubMed: 20649473]
55. Maier CM, Chan PH. Role of superoxide dismutases in oxidative damage and neurodegenerative disorders. Neuroscientist. 2002; 8:323–334. [PubMed: 12194501]
56. Melov S, Coskun PE, Wallace DC. Mouse models of mitochondrial disease, oxidative stress, and senescence. Mutat Res. 1999; 434:233–242. [PubMed: 10486594]
57. Iadecola C, Davisson RL. Hypertension and cerebrovascular dysfunction. Cell Metab. 2008; 7:476–484. [PubMed: 18522829]
58. Jiwa NS, Garrard P, Hainsworth AH. Experimental models of vascular dementia and vascular cognitive impairment: a systematic review. J Neurochem. 2010; 115:814–828. [PubMed: 20731763]
59. Popescu BO, Toescu EC, Popescu LM, Bajenaru O, Muresanu DF, Schultzberg M, et al. Blood-brain barrier alterations in ageing and dementia. J Neurol Sci. 2009; 283:99–106. [PubMed: 19264328]
60. Wiesmann M, Kiliaan AJ, Claassen JA. Vascular aspects of cognitive impairment and dementia. J Cereb Blood Flow Metab. 2013; 33:1696–1706. [PubMed: 24022624]

61. Kolisnyk B, Al-Onaizi MA, Hirata PH, Guzman MS, Nikolova S, Barbash S, et al. Forebrain deletion of the vesicular acetylcholine transporter results in deficits in executive function, metabolic, and RNA splicing abnormalities in the prefrontal cortex. J Neurosci. 2013; 33:14908–14920. [PubMed: 24027290]

62. Prado VF, Roy A, Kolisnyk B, Gros R, Prado MA. Regulation of cholinergic activity by the vesicular acetylcholine transporter. Biochem J. 2013; 450:265–274. [PubMed: 23410039]

63. Bazalakova MH, Blakely RD. The high-affinity choline transporter: a critical protein for sustaining cholinergic signaling as revealed in studies of genetically altered mice. Handb Exp Pharmacol. 2006:525–544. [PubMed: 16722248]

64. Bartus RT, Dean RL 3rd, Beer B, Lippa AS. The cholinergic hypothesis of geriatric memory dysfunction. Science. 1982; 217:408–414. [PubMed: 7046051]

Highlights

- Generation of a novel transgenic mouse model of the “aged brain”
- Expression of HA-tagged $Ca_V1.3$ driven by αCamKII promoter
- Results in ~50% increase in $Ca_V1.3$ channels in forebrain tissue
- Mice exhibit normal behavioral responses in a series of neurobattery tasks

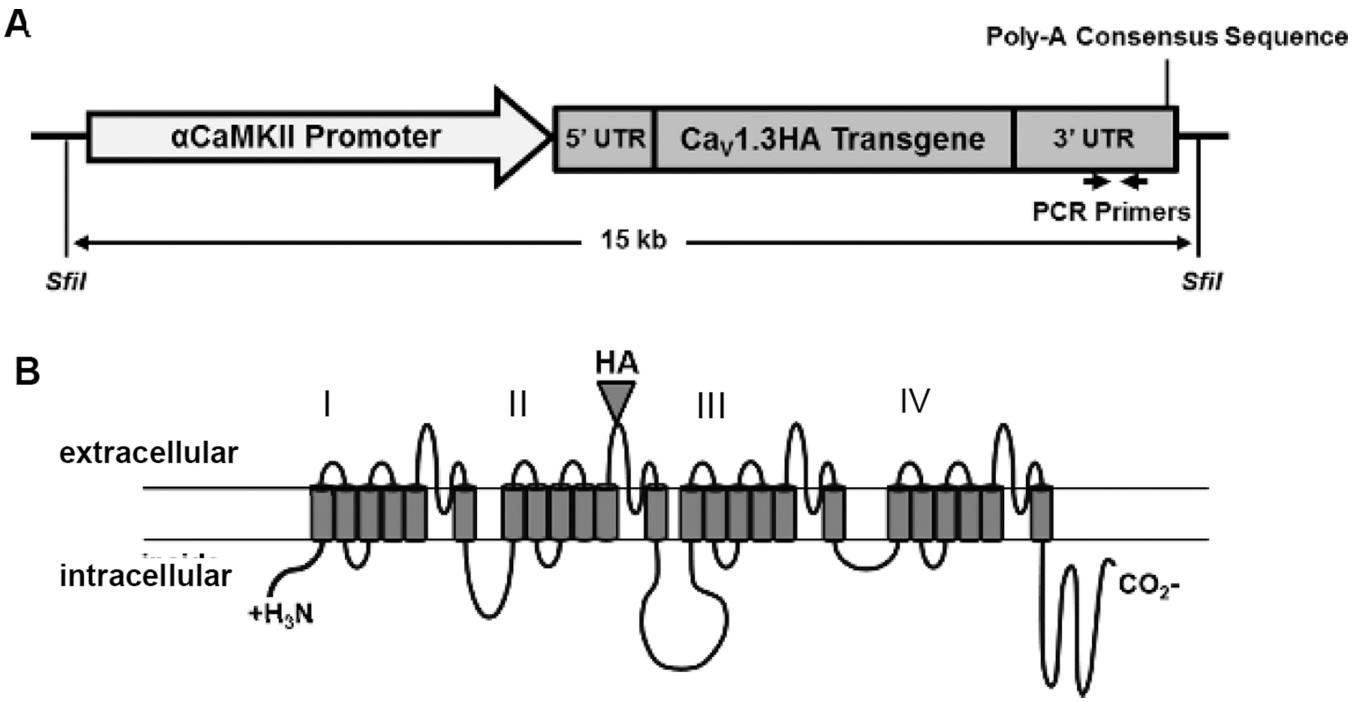

Figure 1. Schematic of injection construct and transgenic protein product

A. Schematic of the linearized injection construct consisting of the αCamKII promoter, $Ca_V1.3$HA cDNA, and the 5' and 3' synthetic UTRs. The 3' UTR includes the location of the forward and reverse primers used in PCR for genotyping mice for the presence of the transgene. **B.** Schematic of the transgenic $Ca_V1.3$HA protein product, including the location of the HA epitope on an extracellular loop of domain II in the four-domain calcium channel.

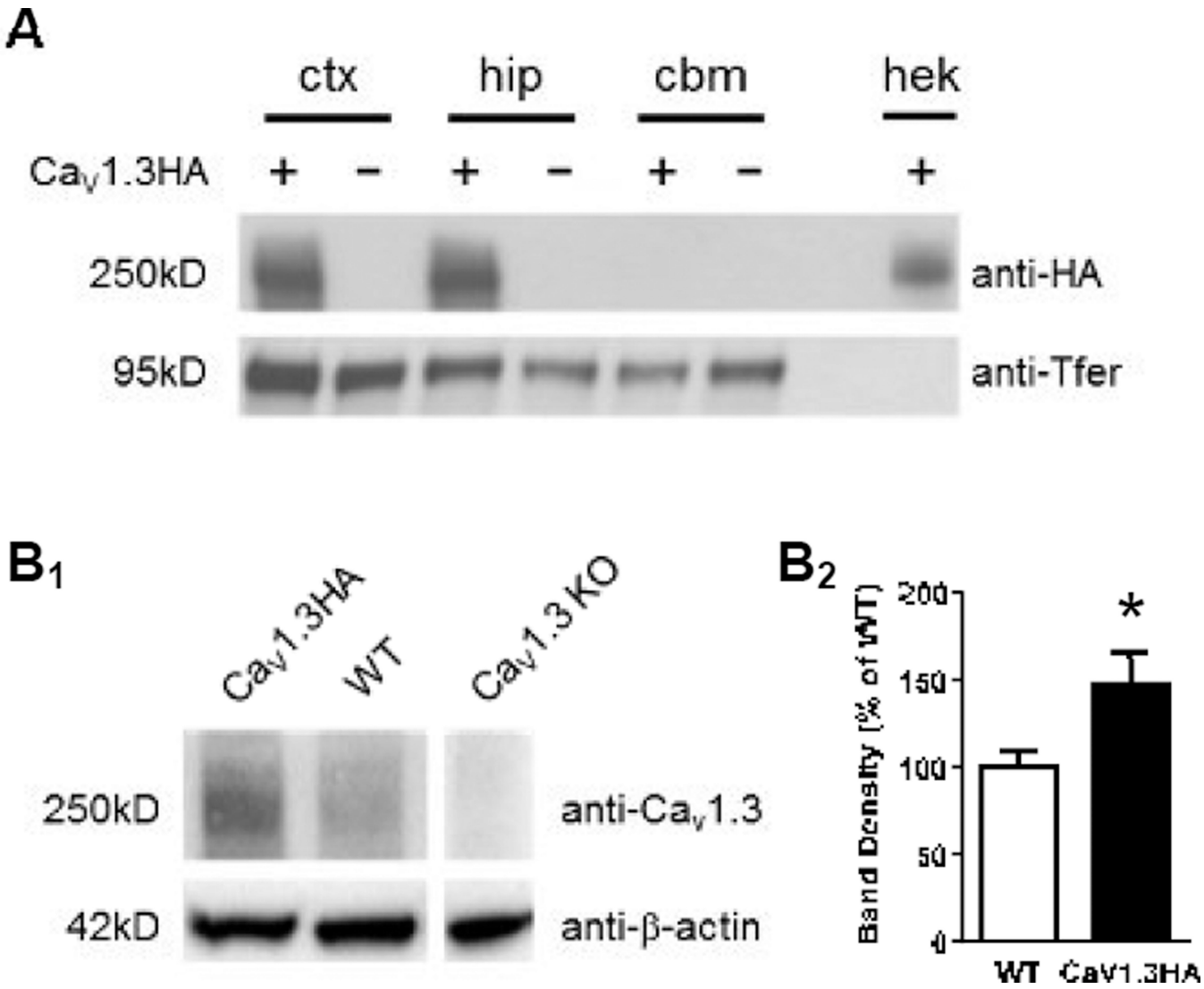

Figure 2. Characterization of transgenic and endogenous $Ca_V1.3$ protein expression in mouse brain

A. Western blot analysis demonstrating specificity of transgenic protein expression. Membrane fractions were prepared from $Ca_V1.3$HA and WT mice and probed with an antibody against the HA epitope (top: mouse anti-HA). A band at approximately 250kD is present in the cortex (ctx) and hippocampus (hip) but not cerebellum (cbm) of $Ca_V1.3$HA but not WT mice, indicating the presence of the transgenic protein. Human embryonic kidney (hek) cells were transfected with the original pCDNA6/V5-hisB/sHA-$Ca_V1.3$a plasmid and used as a positive control for the specificity of the HA antibody. Transferrin (bottom: mouse anti-transferrin antibody [anti-Tfer]) was used as a loading control. **B.** Western blot analysis and quantification of total amount of $Ca_V1.3$ protein (endogenous and transgenic) in $Ca_V1.3$HA and WT mouse brain. **B_1.** A representative example of a Western blot with a whole-brain sample (excluding cerebellum) from one $Ca_V1.3$HA mouse and one WT littermate. Blots were probed with an antibody against $Ca_V1.3$ (top: rabbit anti-1.3) or against β-actin (bottom: rabbit anti-β-actin) as a loading control. Note that a whole-brain

sample from a $Ca_V1.3$ knockout (KO) mouse was also included to ensure specificity of the anti-$Ca_V1.3$ antibody. **B_2.** Whole brain samples were prepared from five $Ca_V1.3$HA and five WT mice. For each animal, the ratio of the $Ca_V1.3$ band density to the β-actin band density was calculated (ImageJ) and then normalized to the average WT band density. The averaged normalized band density of $Ca_V1.3$HA mice was significantly higher than the averaged normalized band density of WT mice (WT = 100.0 ± 9.1%, $Ca_V1.3$HA = 146.9 ± 18.0%, *$p < 0.05$), indicating that $Ca_V1.3$HA mice express approximately 50% more $Ca_V1.3$ than their WT littermates.

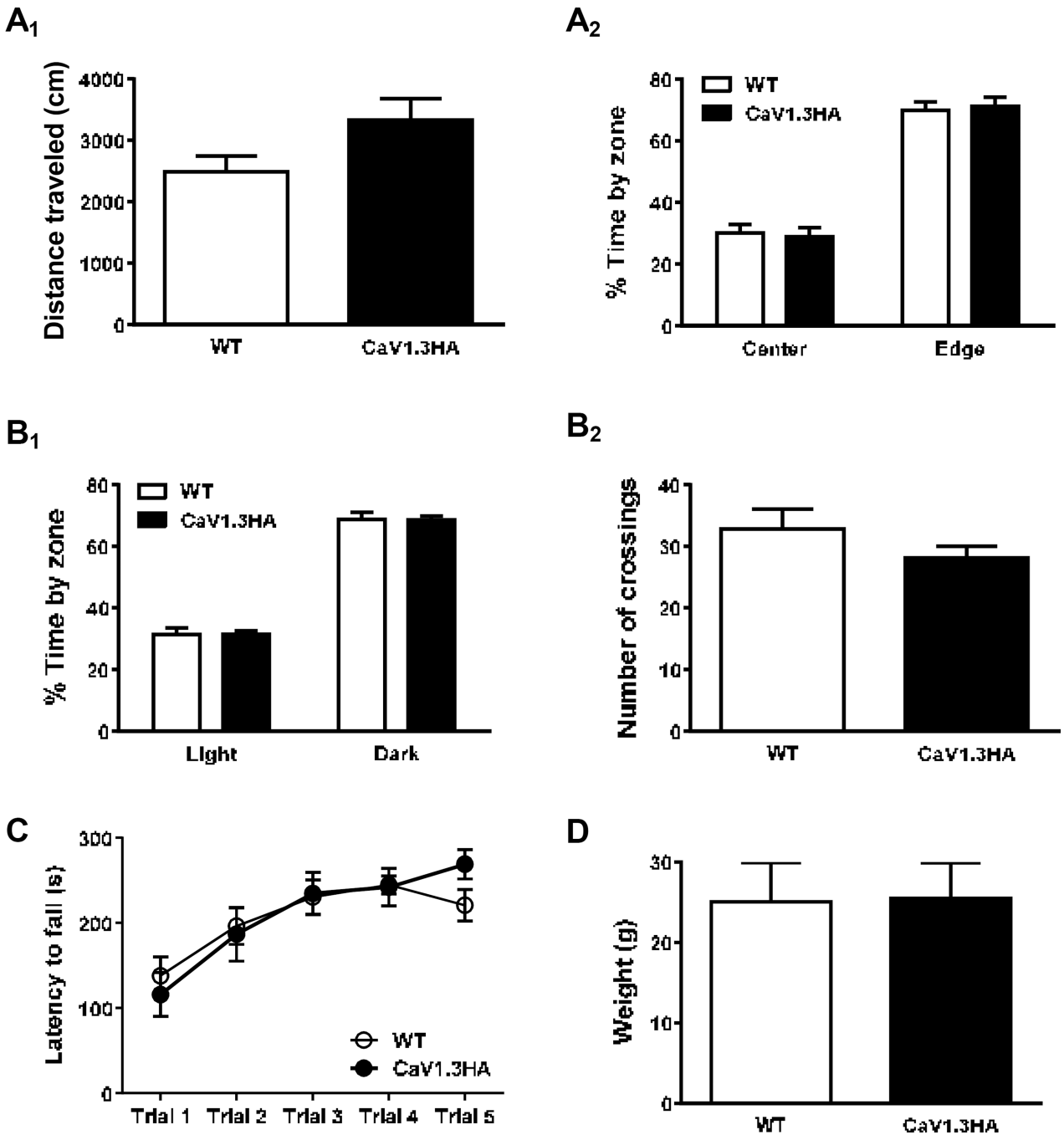

Figure 3. Neurobattery characterization of $Ca_V1.3HA$ and WT littermate mice

A. $Ca_V1.3HA$ (n=13) and WT (n=18) littermate mice were placed individually in an open field for five minutes and the total distance traveled (A_1) and percent time spent in the center and edge zones (A_2) was recorded. There was no significant difference between groups in distance traveled (p=0.06) or the time spent in each zone (p=0.99), although both groups significantly preferred the edge zone to the center (p<0.0001 for both groups). **B.** Mice were placed individually in a light/dark box for five minutes and the percent time spent in the light and dark areas (B_1) as well as the number of crossings between the light and dark sides (B_2)

was recorded. There was no significant difference between genotypes in the number of crossings ($p=0.26$) or the time spent in each area ($p=0.99$), although both groups significantly preferred the dark area to the light ($p<0.0001$ for both groups). **C.** Over the course of one day, mice received 5 trials (inter-trial interval = 1.5hr) on the accelerating rotarod and the latency to fall was recorded (max trial length = 300s). While both groups displayed an increase in latency over the course of training ($p<0.0001$ for both groups), indicative of motor learning, there was no difference in performance between $Ca_V1.3$HA and WT mice ($p=0.87$). **D.** After completion of neurobattery tests, a subset of mice ($Ca_V1.3$HA, n=8; WT, n=5) were weighed; no difference in body weight was observed between $Ca_V1.3$HA and WT mice.

Table 1

Establishment of $Ca_V1.3HA$ transgenic mouse lines

Six pups that were genotyped as positive for the $Ca_V1.3HA$ transgene were received from the University of Michigan Transgenic Core (referred to as “founders”). Each founder was bred with a C57BL/6Tac mouse of the opposite sex to establish a novel mouse line. Lines were then examined for successful breeding (including producing progeny that lived until weaning at 21 days), transmission of the transgene, and production of transgenic protein.

Founding Mouse Number	Sex of Founder	Weaned Progeny?	Transgene in Progeny?	Transgenic Protein in Progeny?
100	Male	**yes**	**yes**	no
101	Male	**yes**	no	n/a
102	Male	**yes**	**yes**	**yes**
103	Male	**yes**	**yes**	**yes**
104	Female	no	n/a	n/a
105	Female	no	n/a	n/a